DYNAMIC AXIAL LOAD TRANSFER FROM ELASTIC BAR TO POROELASTIC MEDIUM

By X. Zeng[1] and R. K. N. D. Rajapakse,[2] Member, ASCE

ABSTRACT: The time-harmonic response of a cylindrical elastic bar (pile) partially embedded in a homogeneous poroelastic medium and subjected to a vertical load is considered. The bar is modeled using 1D elastic theory valid for long bars in the low-frequency range, and the porous medium using Biot's 3D elastodynamic theory. The bar is bonded to the surrounding medium along the contact surface. The problem is formulated by decomposing the bar/porous medium system into a fictitious bar and an extended porous medium. A Fredholm's integral equation of the second kind governs the distribution of axial force in the fictitious bar. The integral equation involves kernels that are displacement and strain influence functions of a poroelastic half-space subjected to a buried, uniform vertical patch load. The governing integral equation is solved by applying numerical quadrature. The solutions for axial displacement and axial force of the bar, and the pore pressure are also derived. Selected numerical results for vertical impedance, axial force, and pore pressure profiles are presented to portray the influence of bar stiffness and length/radius ratio, frequency of excitation, and poroelastic properties.

INTRODUCTION

Muki and Sternberg (1969, 1970) presented the most rigorous mathematical model based on classical theory of elasticity for static axial load transfer from a finite long elastic bar into an elastic half-space. Among others, Freeman and Keer (1967), Luk and Keer (1979), and Karasudhi et al. (1984) presented theoretical studies related to load transfer from an elastic bar into an elastic medium. A variational scheme for static load transfer problems was presented by Selvadurai and Rajapakse (1987). Axial vibrations of an elastic bar partially embedded in an elastic half-space were considered by Fowler and Sinclair (1978), Rajapakse and Shah (1987), and Rajapakse (1988a). Rajapakse (1988b) reviewed literature and the application of classical elasticity to dynamic load transfer problems with an emphasis on the dynamics of elastic piles.

It is well known that fully saturated soils are two-phase materials consisting of soil grains and water. The generation of pore pressure in such two-phase systems under external loading, and the subsequent dissipation of pressure and time-dependent settlement are important aspects in geotechnical engineering applications. Biot (1941) pioneered the development of a 3D theory for fluid-filled elastic porous solids. An elastodynamic theory was later presented by Biot for saturated porous media (Biot 1956). Detournay and Cheng (1991) presented a comprehensive review of poroelasticity.

According to the writers' knowledge, Apirathvorakij and Karasudhi (1980) and Niumpradit and Karasudhi (1981) presented the only theoretical studies dealing with the application of Biot's theory for analysis of the quasi-static response of elastic piles. These writers followed the Muki and Sternberg approach and formulated the load transfer problem in the Laplace transform space. Numerical schemes were used to solve the governing integral equation and to compute inverse Laplace transforms. To our knowledge, no previous study considered the dynamic response of an elastic bar in a poroelastic medium. It is therefore important to examine dynamic load transfer problems within the framework of Biot's theory and to determine the influence of poroelastic effects. Such solutions are important in the theoretical modeling of dynamic response of piles in fluid-saturated soils. Note that numerical approaches, such as the finite-element method, are not the focus of interest in the present study.

In this paper, the writers extend the classical Muki and Sternberg formulation (1970) to analyze steady-state dynamic response of an axially loaded elastic bar partially embedded in a homogeneous poroelastic medium (Fig. 1). Analytical general solutions for Biot's theory are obtained through the application of Hankel integral transforms and they are used in the formulation. A set of influence functions corresponding to a uniform vertical patch load applied in the interior of a half-space is required in the formulation. The load transfer problem is formulated in terms of a Fredholm integral equation of the second kind. The integral equation is solved numerically. Selected numerical results for vertical impedance, axial bar-force, and pore pressure profiles are presented. The influences of the frequency of excitation, bar flexibility, and poroelastic effects on the response are examined.

BASIC EQUATIONS AND INFLUENCE FUNCTIONS

Consider the axisymmetric response of a poroelastic half-space. Let u_i and w_i denote the average displacement of the solid matrix and the fluid displacement relative to the solid matrix, in the i-direction ($i = r, z$), respectively. The constitu-

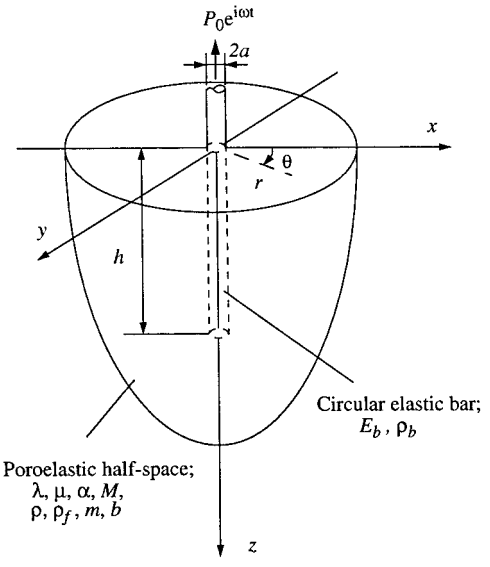

FIG. 1. Geometry of Bar and Embedding Poroelastic Medium

[1]Grad. Student, Civ. and Geological Engrg., Univ. of Manitoba, Canada, R3T 5V6.

[2]Prof., Civ. and Geological Engrg., Univ. of Manitoba, Canada, R3T 5V6.

Note. Associate Editor: Alexander Cheng. Discussion open until February 1, 2000. To extend the closing date one month, a written request must be filed with the ASCE Manager of Journals. The manuscript for this paper was submitted for review and possible publication on November 25, 1998. This paper is part of the ***Journal of Engineering Mechanics***, Vol. 125, No. 9, September, 1999. ©ASCE, ISSN 0733-9399/99/0009-1048–1055/$8.00 + $.50 per page. Paper No. 19715.

J. Eng. Mech., 1999, 125(9): 1048-1055

tive relations of a homogeneous poroelastic material under axisymmetric deformations can be expressed as (Biot 1941)

$$\sigma_{rr} = \lambda e + 2\mu \frac{\partial u_r}{\partial r} - \alpha p_f; \quad \sigma_{\theta\theta} = \lambda e + 2\mu \frac{u_r}{r} - \alpha p_f \tag{1a}$$

$$\sigma_{zz} = \lambda e + 2\mu \frac{\partial u_z}{\partial z} - \alpha p_f; \quad \sigma_{zr} = \mu \left(\frac{\partial u_r}{\partial z} + \frac{\partial u_z}{\partial r} \right) \tag{1b}$$

$$p_f = -\alpha M e + M\varepsilon \tag{1c}$$

where σ_{rr}, $\sigma_{\theta\theta}$, σ_{zz}, and σ_{zr} = total stress component of the bulk material; e and ε = dilatation of the solid phase and the pore fluid, respectively; p_f = excess pore fluid pressure; μ and λ = Lamé's constants of the bulk material; and α and M = Biot's parameters accounting for compressibility of the two-phased material.

The governing equations for axisymmetric motion can be expressed in terms of displacements u_i and w_i ($i = r, z$) (Biot 1962).

$$\mu \nabla^2 u_r + (\lambda + \alpha^2 M + \mu) \frac{\partial e}{\partial r} - \mu \frac{u_r}{r^2} - \alpha M \frac{\partial \varepsilon}{\partial r} = \rho \ddot{u}_r + \rho_f \ddot{w}_r \tag{2a}$$

$$\mu \nabla^2 u_z + (\lambda + \alpha^2 M + \mu) \frac{\partial e}{\partial z} - \alpha M \frac{\partial \varepsilon}{\partial z} = \rho \ddot{u}_z + \rho_f \ddot{w}_z \tag{2b}$$

$$\alpha M \frac{\partial e}{\partial r} - M \frac{\partial \varepsilon}{\partial r} = \rho_f \ddot{u}_r + m\ddot{w}_r + b\dot{w}_r \tag{2c}$$

$$\alpha M \frac{\partial e}{\partial z} - M \frac{\partial \varepsilon}{\partial z} = \rho_f \ddot{u}_z + m\ddot{w}_z + b\dot{w}_z \tag{2d}$$

in which overdots denote the derivatives of field variables with respect to time t; ρ and ρ_f = mass densities of the bulk material and the pore fluid, respectively; $m = \rho_f/\beta$(β = porosity) a density-like parameter; $b = \eta/k$, η fluid viscosity, and k permeability (Biot 1962).

The motion under consideration is assumed to be time-harmonic with a factor of $e^{i\omega t}$, where ω is frequency of the motion and $i = \sqrt{-1}$. For brevity, the term $e^{i\omega t}$ is suppressed from all expressions in the sequel.

The governing equations of motion can be solved by using the Helmholtz representation of a vector field and applying Hankel integral transform with respect to the radial coordinate (Philippacopoulos 1988). The following general solutions for u_r, u_z, and p_f are obtained:

$$u_r = \int_0^\infty [-\xi(Ae^{\gamma_1 z} + Be^{-\gamma_1 z} + Ce^{\gamma_2 z} + De^{-\gamma_2 z}) - \gamma_3(Ee^{\gamma_3 z} - Fe^{-\gamma_3 z})]\xi J_1(\xi r)\, d\xi \tag{3a}$$

$$u_z = \int_0^\infty [\gamma_1(Ae^{\gamma_1 z} - Be^{-\gamma_1 z}) + \gamma_2(Ce^{\gamma_2 z} - De^{-\gamma_2 z}) + \xi(Ee^{\gamma_3 z} + Fe^{-\gamma_3 z})]\xi J_0(\xi r)\, d\xi \tag{3b}$$

$$p_f = \int_0^\infty \mu[\eta_1(Ae^{\gamma_1 z} + Be^{-\gamma_1 z}) + \eta_2(Ce^{\gamma_2 z} + De^{-\gamma_2 z})]\xi J_0(\xi r)\, d\xi \tag{3c}$$

where ξ denotes the Hankel transform parameter; J_0 and J_1 = Bessel functions of the first kind of the zeroth and the first order, respectively; γ_1, γ_2, γ_3, η_1, and η_2 are variables defined in Appendix I; A, B, C, D, E, and F are arbitrary functions to be determined from the boundary conditions.

In the ensuing section dealing with the formulation of the dynamic load transfer problem, a set of influence functions corresponding to a uniform vertical patch load of radius a and of unit intensity, acting in the interior of a poroelastic medium is required. The solution to this problem can be derived by treating the internally loaded half-space as a two-domain boundary-value problem (Karasudhi 1990). The boundary conditions corresponding to the free surface at $z = 0$ ($0 \le r < \infty$) are

$$\sigma_{zn}(r, 0) = 0; \quad n = r, z \tag{4a}$$

$$p_f(r, 0) = 0 \tag{4b}$$

The continuity conditions at the plane of loading, $z = \zeta$($0 \le r < \infty$), are

$$u_n(r, \zeta^+) - u_n(r, \zeta^-) = 0; \quad n = r, z \tag{5a}$$

$$p_f(r, \zeta^+) - p_f(r, \zeta^-) = 0 \tag{5b}$$

$$w_z(r, \zeta^+) - w_z(r, \zeta^-) = 0 \tag{5c}$$

$$\sigma_{zn}(r, \zeta^+) - \sigma_{zn}(r, \zeta^-) = \delta_{zn} H(a - r); \quad n = r, z \tag{5d}$$

where δ_{zn} and H are the Kronecker delta and the Heaviside step function, respectively.

Eqs. (3)–(5) together with the regularity conditions are used to solve the internal loading problem. Explicit solutions for u_r, u_z, and p_f are given by Eqs. (21a)–(21c) in Appendix I.

AXIALLY LOADED BAR IN POROELASTIC MEDIUM

Consider a cylindrical elastic bar of radius a and length h($h/a >> 1$) partially embedded in a poroelastic medium as shown in Fig. 1. The bar is subjected to a time-harmonic axial load $P_0 e^{i\omega t}$ at the top end. The Young's modulus and the mass density of the bar are denoted by E_b and ρ_b, respectively. The material properties of the poroelastic half-space are denoted by λ, μ, α, M, ρ, ρ_f, m, and b as defined previously. The bar is assumed to be fully bonded.

The response of the bar is governed by 1D theory that is applicable to long bars ($h/a >> 1$) excited at low frequencies. Because the bar is elastic, the two limiting cases of hydraulic boundary condition along the contact surface can be either full drainage (zero pore pressure) or zero fluid displacement normal to the contact surface (impermeable). In a practical situation, an intermediate case of nonzero pore pressure and fluid dispacement would exist due to the flow of fluid into the bar (pile). The imposition of an exact hydraulic boundary condition on the bar-medium contact surface is a complex task. Halpern and Christiano (1986) found that negligible difference exists between the vertical compliances and load transfer mechanism of impermeable and fully permeable rigid plates on a poroelastic half-space in the low-frequency range ($\delta = \omega a/\sqrt{\mu/\rho} < 1.0$). In view of the above finding, it is reasonable to assume that the influence of the exact hydraulic boundary condition at the contact surface is not significant on the response. Hence, the present formulation does not impose a hydraulic boundary condition on the contact surface. The pore pressure and normal fluid displacement at the contact surface are nonzero, which is closer to a practical situation and determined according to the decomposition adopted in the study. The consideration of a rigorous hydraulic boundary condition along the contact surface would create substantial difficulties in the theoretical formulation. A rigorous computational approach such as the boundary element method (Cheng et al. 1991) appears to be a more suitable way to consider such a case.

Following Muki and Sternberg (1970), the system shown in Fig. 1 is decomposed into an extended poroelastic half-space H and a fictitious elastic bar B_* (Fig. 2). The material properties of the fictitious bar B_* are characterized by its Young's modulus E_b^* and mass density ρ_b^*, defined as

J. Eng. Mech., 1999, 125(9): 1048-1055

$$E_b^* = E_b - E > 0 \tag{6}$$

$$\rho_b^* = \rho_b - \rho \geq 0 \tag{7}$$

The 1D governing equation for time-harmonic axial motion of the fictitious bar is

$$\frac{d^2 w_b}{dz^2} + k_b^2 w_b + \frac{q}{\pi a^2 E_b^*} = 0 \tag{8}$$

where w_b = axial displacement of the fictitious bar; q = contact force per unit length in the z-direction on the shaft of the bar B_* exerted by H; and $k_b = \omega/c_b$, where $c_b = \sqrt{E_b^*/\rho_b^*}$ is the speed of longitudinal wave in the fictitious bar.

The axial bar-force in B_* can be expressed as

$$p_*(z) = E_b^* \pi a^2 \frac{dw_b}{dz} \tag{9}$$

In addition to the contact shear force q along the shaft, the fictitious bar is also subjected to axial forces $p_*(0)$ and $p_*(h)$, acting on its top and base cross sections, respectivly (Fig. 2).

In contrast to the 1D behavior of B_*, the extended half-space H is treated using the Biot's 3D theory of poroelasticity (Biot 1956). The loading system on the extended poroelastic half-space (Fig. 2) is composed of the contact force $-q(z)/\pi a^2$ distributed uniformly across the cross section D_z, uniform patch load $[P_0 - p_*(0)]/\pi a^2$ acting across D_0 ($z = 0$ and $0 \leq r \leq a$), and a uniformly distributed load $-p_*(h)/\pi a^2$ across D_h ($z = h$ and $0 \leq r \leq a$).

To determine the unknown forces $p_*(0)$, $p_*(h)$, and $q(z)$, a suitable compatibility condition between B_* and H must be imposed. Muki and Sternberg (1970) adopted the condition that the axial strain of the fictitious bar be equal to the average of the extensional strain ε_{zz} of the cross section D_z of the extended half space. Fowler and Sinclair (1978) employed the condition that the vertical displacement of B_* be equal to the average vertical displacement of D_z for $0 \leq z \leq h$. Rajapakse (1988*a*,*b*) made a comprehensive investigation on the compatibility condition for dynamic load transfer problems for elastic media. It was found that the bond condition should be based on the compatibility of vertical displacement along the edge of D_z. This condition gave the most accurate solutions when applied to the limiting case of a rigid bar for which a rigorous numerical solution can be obtained using the boundary element method. Therefore, in the present study $p_*(z)$ is determined on the condition that the vertical displacement of B_* is equal to that of D_z at $r = a$ for $0 \leq z \leq h$.

With the aid of displacement and strain influence functions corresponding to a buried uniform vertical load, the vertical displacement and the vertical extensional strain of D_z at depth z and $r = a$ are given by

$$w(z) = \frac{1}{\pi a^2}([P_0 - p_*(0)]\hat{w}(z, 0) + p_*(h)\hat{w}(z, h) + \int_0^h q(\zeta)\hat{w}(z, \zeta)\, d\zeta) \tag{10}$$

$$\gamma(z) = \frac{1}{\pi a^2}([P_0 - p_*(0)]\hat{\gamma}(z, 0) + p_*(h)\hat{\gamma}(z, h) + \int_0^h q(\zeta)\hat{\gamma}(z, \zeta)\, d\zeta) \tag{11}$$

in which $\hat{w}$ and $\hat{\gamma}$ are the displacement and the strain influence functions given by (27) and (28) in Appendix I, respectively.

Manipulation of (8)–(11) together with the displacement compatibility condition described above results in the following Fredholm's integral equation of the second kind for the nondimensionalized fictitious bar-force $\bar{p}_*(z)$ ($=p_*(z)/P_0$)

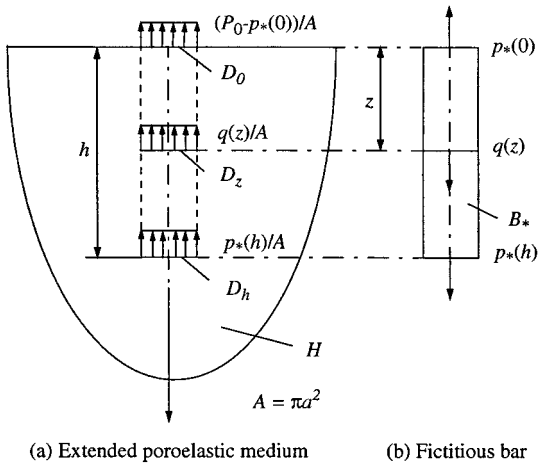

FIG. 2. Decomposition of Elastic Bar/Poroelastic Half-Space

$$\left[\frac{1}{E_b^*} + 2\hat{\gamma}_1(z, z)\right]\bar{p}_*(z) = \hat{\gamma}(z, 0) + \int_0^h \left[\bar{p}_*(\zeta)\frac{\partial \hat{\gamma}}{\partial \zeta}(z, \xi) + k_b^2 \hat{\gamma}(z, \zeta)\int_\zeta^h \bar{p}_*(\eta)\, d\eta\right] d\zeta - \Delta \int_0^h \hat{\gamma}(z, \zeta)\, d\zeta \left\{\hat{w}(h, 0) + \int_0^h \cdot \left[\bar{p}_*(\zeta)\frac{\partial \hat{w}}{\partial \zeta}(h, \zeta) + k_b^2 \hat{w}(h, \zeta)\int_\zeta^h \bar{p}_*(\eta)\, d\eta\right] d\zeta\right\} \tag{12}$$

where

$$\Delta = \left[\frac{1}{k_b^2 E_b^*} + \int_0^h \hat{w}(h, \zeta)\, d\zeta\right]^{-1} \tag{13}$$

and $\hat{\gamma}_1$ is a function [(30) in Appendix I] accounting for the discontinuity in the strain influence function.

Once the fictitious bar force $\bar{p}_*(z)$ is known, the axial displacement of the bar can be determined by

$$w(z) = \frac{P_0 \Delta}{\pi a^2 k_b^2 E_b^*}\left(\hat{w}(h, 0) + \int_0^h \left(\bar{p}_*(\zeta)\frac{\partial \hat{w}}{\partial \zeta}(h, \zeta) + k_b^2 \hat{w}(h, \zeta)\int_\zeta^h \bar{p}_*(\eta)\, d\eta\right) d\zeta\right) - \frac{P_0}{\pi a^2 E_b^*}\int_z^h \bar{p}_*(\zeta)\, d\zeta \tag{14}$$

The real bar force $p(z)$ is determined by adding the fictitious bar-force and the resultant force of stress σ_{zz} over the cross section D_z of H. The axial force of the real bar is therefore given by

$$p(z) = p_*(z) + \frac{1}{\pi a^2}\left([P_0 - p_*(0)]\hat{\sigma}(z, 0) + p_*(h)\hat{\sigma}(z, h) + \int_0^h q(\zeta)\hat{\sigma}(z, \zeta)\, d\zeta\right) \tag{15}$$

in which $\hat{\sigma}$ = influence function for vertical stress as given by (31) in Appendix I.

The pore pressure generated in the poroelastic medium due to dynamic axial loading can be determined by using an approach identical to the axial bar force. The average pore pressure generated in the medium for $0 \leq z \leq h$ can be expressed as

J. Eng. Mech., 1999, 125(9): 1048-1055

$$p_f^a(z) = \frac{1}{\pi a^2}\left([P_0 - p_*(0)]\,\widehat{p_f^a}(z, 0) + p_*(h)\,\widehat{p_f^a}(z, h) + \int_0^h q(\zeta)\,\widehat{p_f^a}(z, \zeta)\,d\zeta\right) \tag{16}$$

where $\widehat{p_f^a}$ = influence function for average pore pressure defined by (33) in Appendix I.

The Fredholm integral equation [(12)] governing the fictitious bar force $\bar{p}_*(z)$ can be solved numerically by the following procedure. The range of integration [0, h] is subdivided into N equally spaced elements, and $\bar{p}_*(z)$ is approximated by a continuous piecewise linear function. In the numerical solution, it is demanded that (12) holds at the nodal points of each of the elements and the trapezoidal rule to evaluate the single and double integrals will be employed. Note that integrals along the elements, hence along the bar, can be obtained analytically through a permissible interchange in the order of integration, but the remaining semi-infinite integrals involved in the influence functions are computed by employing numerical quadrature. In the numerical solution, the Fredholm integral equation is reduced to a set of linear simultaneous equations with the nodal fictitious bar forces as the unknowns. Once the nodal fictitious bar forces are determined, the axial displacement, the axial force of the elastic bar, and the pore pressure are evaluated by applying a numerical quadrature to (14)–(16), respectively.

NUMERICAL RESULTS AND DISCUSSIONS

The following dimensionless quantities, namely, the normalized axial impedance $\bar{K}_v$, flexibility ratio $\bar{E}$, mass density ratio $\bar{\rho}$, length/radius ratio $\bar{h}$, normalized bar force $\bar{p}(z)$, and the normalized average pore pressure $\overline{p_f^a}$ are used in the numerical study

$$\bar{K}_v = \frac{P_0}{\mu a w(0)}, \quad \bar{E} = \frac{E_b}{E}, \quad \bar{\rho} = \frac{\rho_b}{\rho}, \quad \bar{h} = \frac{h}{a}, \quad \bar{p}(z) = \frac{p(z)}{P_0}, \quad \overline{p_f^a} = \frac{\pi a^2 p_f^a(z)}{P_0} \tag{17}$$

where E = drained Young's modulus of the bulk material of a poroelastic medium.

A study was initially conducted to determine the stability and convergence of the numerical solutions with respect to the number of node points N used to discretize (12). It is found that solutions for $\bar{p}_*(z)$ converge for N = 10–15, in the nondimensional frequency range $0 < \delta < 0.5$ and for the bar length/radius ratio $\bar{h} \le 30$. All numerical solutions correspond to N = 10 for $\bar{h} \le 20$ and N = 15 for $\bar{h}$ = 30.

The overall accuracy of the formulation and the numerical implementation is investigated by comparing with the elastostatic load-transfer case of Muki and Sternberg (1970), and its elastodynamic counterpart reported by Rajapakse (1988a). Fig. 3 shows a comparison of present solutions for $\bar{p}(z)$ for the static case with those reported by Muki and Sternberg (1970). The results in Fig. 3 are obtained by the degeneration of a poroelastic medium to an ideal elastic medium (the values of M^*, ρ^*, m^*, b^*, and α are set to 0.0001). The two sets of solutions agree very closely. Table 1 presents a comparison of solutions for vertical impedance $\bar{K}_v$ for steady-state dynamic problems for ideal elastic media with solutions reported by Rajapakse (1988a) using a variational scheme. The accuracy of the present formulation and its numerical implementation are confirmed by the above comparisons.

In the remainder of this paper, the influence of frequency of excitation, bar flexibility ratio, bar length/radius ratio, and poroelastic material properties on the dynamic response are investigated. Three poroelastic materials are considered in the analysis, the nondimensional properties are $\lambda^* = 1.5$, $M^* = 12.2$, $\rho^* = 0.53$, $m^* = 1.1$, and $\alpha = 0.97$, with $b^* = 0$, 50, and 1,000, respectively. It is anticipated that among the different poroelastic properties, b^* should have the most influence on the response because it reflects the potential of diffusivity of the material (k, permeability).

Fig. 4 shows the vertical impedance of an elastic bar embedded in an ideal elastic medium ($\lambda^* = 1.5$, $\nu = 0.3$) and two of the above poroelastic materials with $b^* = 0$ and 1,000. The solutions correspond to bar properties: $\bar{E}$ = 1,000, $\bar{\rho}$ = 1.2, and $\bar{h}$ = 20. The real part of vertical impedance does not show large variations with the frequency in the range $\delta = 0.0$–0.5 for all three materials. The poroelastic medium with a larger value of b^* shows slightly higher stiffness. The imaginary part

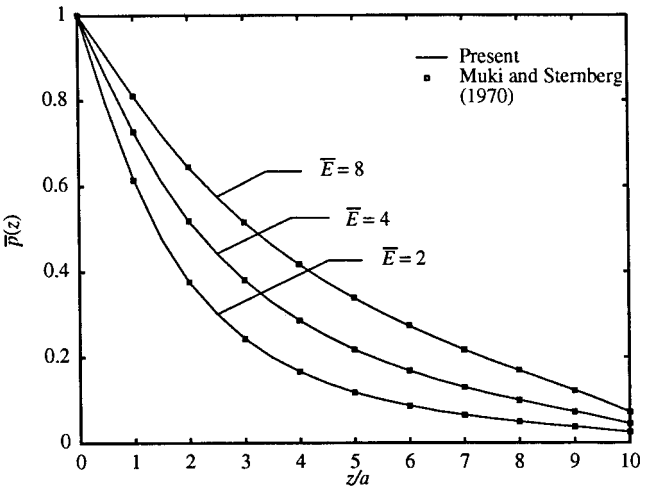

FIG. 3. Profile of Axial Force of Elastic Bar for Static Ideal Elastic Case ($\bar{h}$ = 10, ν = 0.25)

TABLE 1. Comparison of Dimensionless Vertical Impedance for Elastic Bar Embedded In Elastic Medium[a]

$\bar{E}$ (1)	Rajapakse and Shah (1987) (2)	Rajapakse (1988a) (3)	Present study (4)
10.0	(14.35, 8.40)	(14.36, 8.29)	(14.31, 8.10)
50.0	(23.16, 21.31)	(23.20, 20.89)	(23.17, 20.08)
100.0	(24.06, 25.00)	(24.68, 26.04)	(24.75, 25.06)
1000.0	(24.31, 32.81)	(25.24, 32.81)	(25.45, 31.69)

[a] $\bar{h}$ = 10.0, $\bar{\rho}$ = 1.0, ν = 0.25, and δ = 0.4.

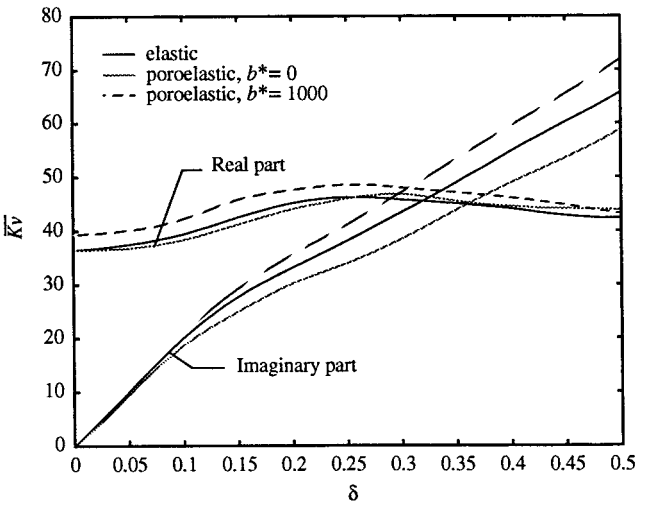

FIG. 4. Vertical Impedance of Elastic Bar in Poroelastic Medium ($\bar{h}$ =, $\bar{\rho}$ = 1.2)

J. Eng. Mech., 1999, 125(9): 1048-1055

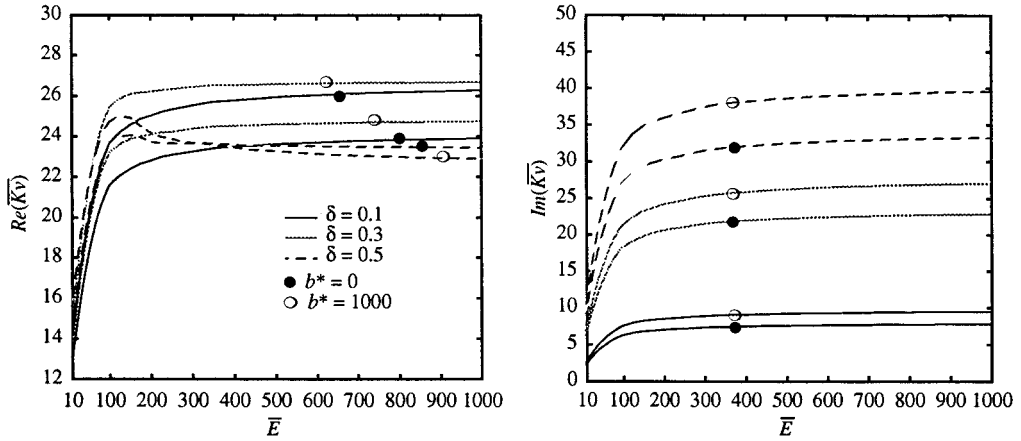

FIG. 5. Variation of Vertical Impedance of Elastic Bar with $\bar{E}$ ($\bar{h}$ = 10, $\bar{\rho}$ = 1.2)

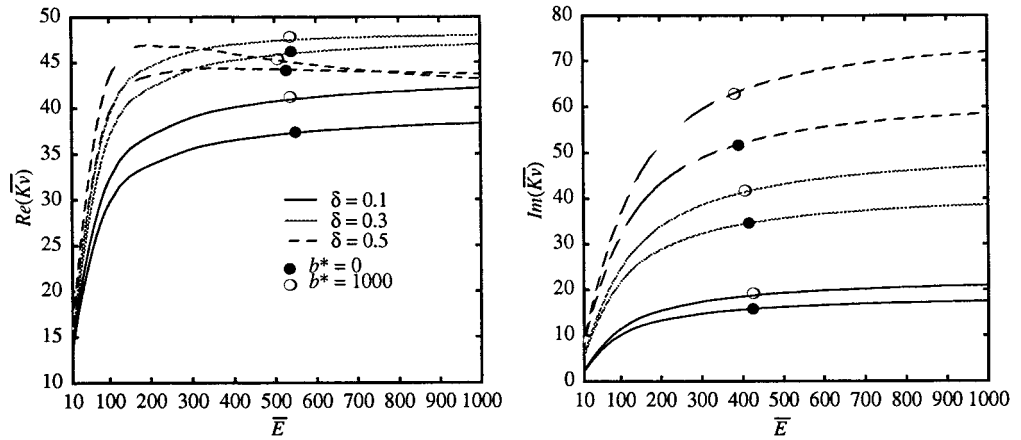

FIG. 6. Variation of Vertical Impedance of Elastic Bar with $\bar{E}$ ($\bar{h}$ = 20, $\bar{\rho}$ = 1.2)

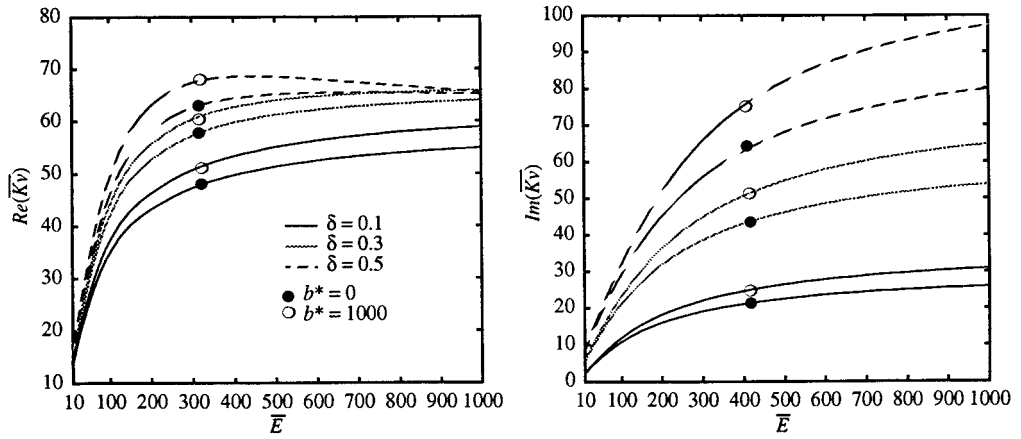

FIG. 7. Variation of Vertical Impedance of Elastic Bar with $\bar{E}$ ($\bar{h}$ = 30, $\bar{\rho}$ = 1.2)

of vertical impedance shows strong dependence on the frequency and the type of surrounding medium. An increase (more damping) in the value of $Im(K_v)$ is noted with increasing b^*. However, $Im(K_v)$ shows negligible changes for $b^* > 1{,}000$ when compared with $b^* = 1{,}000$. Generally, materials such as sands have a low value of b^*, and clays have larger values of b^* $[=(\eta/k)(a/\sqrt{\rho\mu})]$. The pore pressure dissipation is slower and poroelastic effects are more dominant in clays than in sands.

The influence of bar flexibility ratio $\bar{E}$ and δ on the vertical impedance is shown in Figs. 5–7 for $\bar{h}$ = 10, 20, and 30, respectively. The two poroelastic materials with $b^* = 0$ and 1,000 are used in the analysis. As expected, both real part and imaginary parts of vertical impedance show initially a steep increase with bar flexibility ratio and then reach an asymptotic value corresponding to a practically rigid bar. Note that $\bar{E}$ corresponding to the rigid bar limit is dependent on the length/radius ratio and slightly on the frequency of excitation. The impedance shows dependence on the frequency of excitation and b^*. The influence of b^* is more dominant on the imaginary part when compared with the real part of the vertical impedance. It is also noted that the influence of b^* is more significant at higher frequencies and for relatively rigid bars. Additional numerical studies indicated that the effect of bar

J. Eng. Mech., 1999, 125(9): 1048-1055

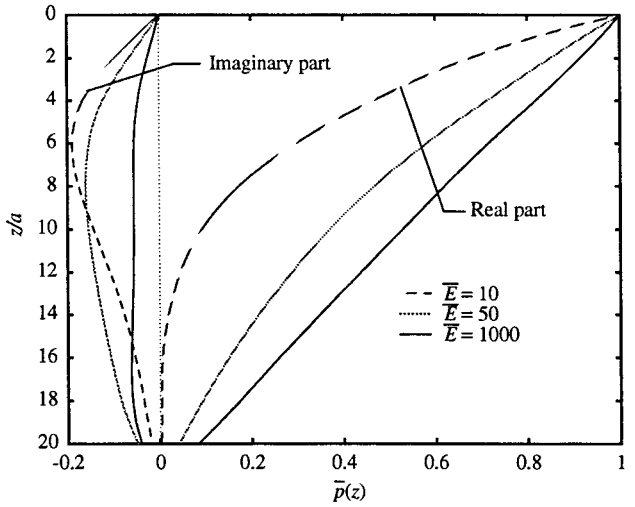

FIG. 8. Profile of Axial Force of Elastic Bar in Poroelastic Medium for Various $\bar{E}$ (h = 20, $\bar{\rho}$ = 1.2)

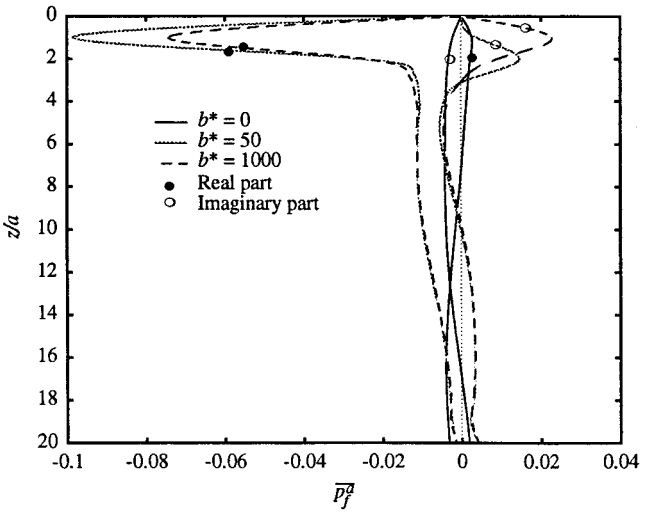

FIG. 9. Variation of Average Pore Pressure along Elastic Bar ($\bar{h}$ = 20, $\bar{\rho}$ = 1.2)

density ratio $\bar{\rho}$ is negligible over the low-frequency range considered in this study.

Fig. 8 shows the profiles of nondimensional axial force $\bar{p}(z)$ along the length of a bar with properties $\bar{h}$ = 20.0, $\bar{\rho}$ = 1.2, and b^* = 1,000 for δ = 0.5. The bar-force profiles have a significant dependence on bar stiffness ratio $\bar{E}$. The load transfer along the bar is rapid for smaller values of $\bar{E}$, resulting in negligible load transfer at the base. For stiffer bars, the load transfer is more gradual and a part of the load is carried to the base. The influence of b^* on the bar-force profiles is found to be relatively small. Fig. 9 shows the profile of nondimensional average pore pressure $\bar{p}_f^a$ along the bar length with the dimensionless quantity b^*. The properties of the bar are $\bar{h}$ = 20.0, $\bar{E}$ = 10.0, $\bar{\rho}$ = 1.2, and δ = 0.5. Pore pressure generation is mostly confined to the upper part of the bar. The peak nondimensional pore pressure is only a fraction of the load applied to the bar. As expected, the pore pressure is higher for a medium with a larger b^* that is smaller permeability. Additional numerical results show an increase in pore pressure magnitude with increasing bar stiffness.

CONCLUSIONS

The Muki and Sternberg formulation is successfully extended here to analyze the time-harmonic response of an axially loaded elastic cylindrical bar partially embedded in a homogeneous poroelastic medium. The problem is formulated by using analytical solutions for displacement and strain influence functions of a poroelastic half-space subjected to buried dynamic loading. A Fredholm's integral equation of the second kind governs the axial force in the fictitious bar. The integral equation can be accurately solved by using numerical quadrature. The stability and convergence of the numerical implementation were confirmed. The present solutions agree very closely with existing solutions for static and dynamic problems involving ideal elastic materials. Numerical solutions for vertical impedance of elastic bars embedded in poroelastic media show strong dependence on the frequency of excitation, the fluid viscosity and the permeability of the medium, bar stiffness ratio, and the bar length/radius ratio. Axial load transfer profiles show strong dependence on the bar stiffness ratio and frequency of excitation. Pore pressure profiles also show strong dependence on the fluid viscosity and the permeability of the medium. The solution presented here is apparently the first theoretical study of dynamic response of an elastic pile in a poroelastic soil. Solutions for layered systems can be developed by simply using appropriate influence functions. The method can also be extended to consider the dynamic response of laterally loaded piles in fully saturated soils.

APPENDIX I

For convenience, the material properties λ, M, ρ_f, m, and b of a poroelastic medium and the frequency of excitation ω are nondimensionalized as

$$\lambda^* = \frac{\lambda}{\mu}; \quad M^* = \frac{M}{\mu}; \quad \rho^* = \frac{\rho_f}{\rho}; \quad m^* = \frac{m}{\rho} \qquad (18a\text{–}d)$$

$$b^* = \frac{ab}{\sqrt{\rho\mu}}; \quad \delta = \sqrt{\frac{\rho}{\mu}}\,\omega a \qquad (18e,f)$$

The variables γ_i (i = 1, 2, 3) and η_i (i, = 1, 2) appearing in (3) are defined as

$$\gamma_i = \sqrt{\xi^2 - L_i^2}, \quad i = 1, 2; \quad \gamma_3 = \sqrt{\xi^2 - S^2} \qquad (19a)$$

$$\eta_i = (\alpha + \chi_i)M^*L_i^2, \quad i = 1, 2 \qquad (19b)$$

where

$$\chi_i = \frac{(\lambda^* + \alpha^2 M^* + 2)L_i^2 - \delta^2}{\rho^*\delta^2 - \alpha M^* L_i^2}, \quad i = 1, 2 \qquad (20a)$$

$$L_1^2 = \frac{w_1 + \sqrt{w_1^2 - 4w_2}}{2}; \quad L_2^2 = \frac{w_1 - \sqrt{w_1^2 - 4w_2}}{2} \qquad (20b)$$

$$S^2 = (\rho^*\chi_3 + 1)\delta^2 \qquad (20c)$$

$$w_1 = \frac{(m^*\delta^2 - ib^*\delta)(\lambda^* + \alpha^2 M^* + 2) + M^*\delta^2 - 2\alpha M^*\rho^*\delta^2}{(\lambda^* + 2)M^*} \qquad (20d)$$

$$w_2 = \frac{(m^*\delta^2 - ib^*\delta)\delta^2 - (\rho^*)^2\delta^4}{(\lambda^* + 2)M^*} \qquad (20e)$$

$$\chi_3 = \frac{\rho^*\delta}{ib^* - m^*\delta} \qquad (20f)$$

The following solutions for radial and vertical displacements and excess pore pressure are obtained for a poroelastic half-space subjected to a uniform circular vertical load at $z = \zeta$

$$u_r(r, z, \zeta) = \int_0^\infty [F_1(\xi, z, \zeta) + F_2(\xi, z, \zeta)]aJ_1(\xi a)J_1(\xi r)\, d\xi \qquad (21a)$$

$$u_z(r, z, \zeta) = \int_0^\infty [F_3(\xi, z, \zeta) + F_4(\xi, z, \zeta)]aJ_1(\xi a)J_0(\xi r)\, d\xi \qquad (21b)$$

J. Eng. Mech., 1999, 125(9): 1048-1055

$$p_f(r, z, \zeta) = \int_0^\infty [F_5(\xi, z, \zeta) + F_6(\xi, z, \zeta)] a J_1(\xi a) J_0(\xi r)\, d\xi \quad (21c)$$

where

$$F_1(\xi, z, \zeta) = -\xi(A_0 e^{-\gamma_1|z-\zeta|} + C_0 e^{-\gamma_2|z-\zeta|}) - \gamma_3 E_0 e^{-\gamma_3|z-\zeta|} \quad (22a)$$

$$F_2(\xi, z, \zeta) = -\xi(B_0 e^{-\gamma_1 z} + D_0 e^{-\gamma_2 z}) + \gamma_3 F_0 e^{-\gamma_3 z} \quad (22b)$$

$$F_3(\xi, z, \zeta) = \gamma_1 A_0 e^{-\gamma_1|z-\zeta|} + \gamma_2 C_0 e^{-\gamma_2|z-\zeta|} + \xi E_0 e^{-\gamma_3|z-\zeta|} \quad (22c)$$

$$F_4(\xi, z, \zeta) = -\gamma_1 B_0 e^{-\gamma_1 z} - \gamma_2 D_0 e^{-\gamma_2 z} + \xi F_0 e^{-\gamma_3 z} \quad (22d)$$

$$F_5(\xi, z, \zeta) = \mu(\eta_1 A_0 e^{-\gamma_1|z-\zeta|} + \eta_2 C_0 e^{-\gamma_2|z-\zeta|}) \quad (22e)$$

$$F_6(\xi, z, \zeta) = \mu(\eta_1 B_0 e^{-\gamma_1 z} + \eta_2 D_0 e^{-\gamma_2 z}) \quad (22f)$$

$$A_0 = -\frac{\eta_2}{2\mu N_1}, \quad B_0 = -\frac{\eta_2(v_5 e^{-\gamma_1\zeta} + 2\xi^2 v_3 e^{-\gamma_2\zeta} - 4\xi^2 S_1 v_1 e^{-\gamma_3\zeta})}{2\mu N_1 R} \quad (23a)$$

$$C_0 = \frac{\eta_1}{2\mu N_1}, \quad D_0 = -\frac{\eta_1(2\xi^2 v_4 e^{-\gamma_1\zeta} - v_6 e^{-\gamma_2\zeta} + 4\xi^2 S_1 v_1 e^{-\gamma_3\zeta})}{2\mu N_1 R} \quad (23b)$$

$$E_0 = -\frac{\xi v_1}{2\mu\gamma_3 N_1}, \quad F_0 = -\frac{\xi v_2(v_4 e^{-\gamma_1\zeta} - v_3 e^{-\gamma_2\zeta}) + \xi v_1 v_7 e^{-\gamma_3\zeta}}{2\mu\gamma_3 N_1 R} \quad (23c)$$

$$v_1 = \eta_1 - \eta_2; \quad v_2 = \eta_1\beta_2 - \eta_2\beta_1; \quad v_3 = 4\eta_1\gamma_2\gamma_3 \quad (24a\text{–}c)$$

$$v_4 = 4\eta_2\gamma_3\gamma_1; \quad \beta_i = 2\gamma_i^2 - \lambda^* L_i^2 - \alpha\eta_i, \quad i = 1, 2 \quad (24d,e)$$

$$v_5 = S_1 v_2 - \xi^2(v_3 + v_4); \quad v_6 = S_1 v_2 + \xi^2(v_3 + v_4) \quad (25a,b)$$

$$v_7 = S_1 v_2 + \xi^2(v_3 - v_4) \quad (25c)$$

$$S_1 = \xi^2 + \gamma_3^2; \quad N_1 = 2\xi^2 v_1 - v_2 \quad (26a,b)$$

$$R = -S_1 v_2 + \xi^2(v_3 - v_4) \quad (26c)$$

The displacement influence function $\hat{w}$ can be expressed as

$$\hat{w}(z, \zeta) = u_z(a, z, \zeta) = \int_0^\infty [F_3(\xi, z, \zeta) + F_4(\xi, z, \zeta)] a J_1(\xi a) J_0(\xi a)\, d\xi \quad (27)$$

The strain influence function $\hat{\gamma}$ is given by

$$\hat{\gamma}(z, \zeta) = \frac{\partial \hat{w}}{\partial z}(z, \zeta) = \int_0^\infty [F_7(\xi, z, \zeta) + F_8(\xi, z, \zeta)] a J_1(\xi a) J_0(\xi a)\, d\xi \quad (28)$$

in which

$$F_7(\xi, z, \zeta) = \mathrm{sgn}(z - \zeta)[-\gamma_1^2 A_0 e^{-\gamma_1|z-\zeta|} - \gamma_2^2 C_0 e^{-\gamma_2|z-\zeta|} - \xi\gamma_3 E_0 e^{-\gamma_3|z-\zeta|}] \quad (29a)$$

$$F_8(\xi, z, \zeta) = \gamma_1^2 B_0 e^{-\gamma_1 z} + \gamma_2^2 D_0 e^{-\gamma_2 z} - \xi\gamma_3 F_0 e^{-\gamma_3 z} \quad (29b)$$

and sgn = signum function.

The term relating to the discontinuity of the strain influence function is defined as

$$\hat{\gamma}_1(z, \zeta) = \int_0^\infty \frac{F_7(\xi, |z - \zeta|)}{\mathrm{sgn}(z - \zeta)} a J_1(\xi a) J_0(\xi a)\, d\xi \quad (30)$$

The stress influence function $\hat{\sigma}$ defined as the integration of vertical stress σ_{zz} over a circular disk ($0 \le r \le a$) at depth z is given by

$$\hat{\sigma}(z, \zeta) = 2\pi a^2 \int_0^\infty [F_9(\xi, z, \zeta) + F_{10}(\xi, z, \zeta)] \frac{J_1^2(\xi a)}{\xi}\, d\xi \quad (31)$$

in which

$$F_9(\xi, z, \zeta) = -\mathrm{sgn}(z - \zeta)[\mu\beta_1 A_0 e^{-\gamma_1|z-\zeta|} + \mu\beta_2 C_0 e^{-\gamma_2|z-\zeta|} + 2\mu\xi\gamma_3 E_0 e^{-\gamma_3|z-\zeta|}] \quad (32a)$$

$$F_{10}(\xi, z, \zeta) = \mu\beta_1 B_0 e^{-\gamma_1 z} + \mu\beta_2 D_0 e^{-\gamma_2 z} - 2\mu\xi\gamma_3 F_0 e^{-\gamma_3 z} \quad (32b)$$

The influence function $\widehat{p_f^a}$ for the average pore pressure is defined as the average of pore pressure p_f over a circular disk ($0 \le r \le a$) at depth z and expressed in the form

$$\widehat{p_f^a}(z, \zeta) = \int_0^\infty [F_{11}(\xi, z, \zeta) + F_{12}(\xi, z, \zeta)] \frac{J_1^2(\xi a)}{\xi}\, d\xi \quad (33)$$

where

$$F_{11}(\xi, z, \zeta) = 2\mu(\eta_1 A_0 e^{-\gamma_1|z-\zeta|} + \eta_2 C_0 e^{-\gamma_2|z-\zeta|}) \quad (34a)$$

$$F_{12}(\xi, z, \zeta) = 2\mu(\eta_1 B_0 e^{-\gamma_1 z} + \eta_2 D_0 e^{-\gamma_2 z}) \quad (34b)$$

The displacement, strain, stress, and pore pressure influence functions given above appear in terms of semi-infinite integrals. These integrals cannot be evaluated analytically. All influence functions required in the solution are evaluated by using the numerical quadrature subroutine DQDAG of IMSL (*IMSL* 1989).

ACKNOWLEDGMENTS

The work presented in this paper was supported by the Natural Sciences and Engineering Council of Canada, Grant A-6507.

APPENDIX II. REFERENCES

Apirathvorakij, V. and Karasudhi, P. (1980). ''Quasicstatic bending of a cylindrical elastic bar partially embedded in a saturated elastic half space.'' *Int. J. Solids and Struct.*, 16, 625–644.

Biot, M. A. (1941). ''General theory of three-dimensional consolidation.'' *J. Appl. Phys.*, 12, 155–164.

Biot, M. A. (1956a). ''Theory of propagation of elastic waves in a fluid-saturated porous solid. I: Low frequency range.'' *J. Acoust. Soc. Am.*, 28, 168–178.

Biot, M. A. (1956b). ''Theory of propagation of elastic waves in a fluid-saturated porous solid. II: High frequency range.'' *J. Acoust. Soc. Am.*, 28, 179–191.

Biot, M. A. (1962). ''Mechanics of deformation and acoustic propagation in porous media.'' *J. Appl. Phys.*, 33, 1482–1498.

Cheng, A. H.-D., Badmus, T., and Beskos, D. E. (1991). ''Integral equation for dynamic poroelasticity in frequency domain with BEM solution.'' *J. Engrg. Mech.*, ASCE, 117, 1136–1157.

Detournay, E., and Cheng, A. H. D. (1991). ''Fundamentals of poroelasticity.'' *Comprehensive rock engineering: Principles, practice and projects*, Vol. 2, Pergamon, Oxford, England.

Fowler, G. F., and Sinclair, G. B. (1978). ''The longitudinal harmonic excitation of a circular bar embedded in an elastic half-space.'' *Int. J. Solids and Struct.*, 14, 999–1012.

Freeman, N. J., and Keer, L. M. (1967). ''Torsion of a cylindrical rod welded to an elastic half space.'' *J. Appl. Mech.*, 34, 687–692.

Halpern, M. R., and Christiano, P. (1986). ''Steady-state harmonic response of a rigid plate bearing on a liquid-saturated poroelastic half-space.'' *Earthquake Engrg. Struct. Dyn.*, 14, 439–454.

IMSL MATH/LIBRARY: FORTRAN subroutines for mathematical applications, version 1.1. (1989). IMSL Inc., Houston.

Karasudhi, P. (1990). *Foundation of solid mechanics.* Kluwer, Dordrecht, The Netherlands.

Karasudhi, P., Rajapakse, R. K. N. D., and Hwang, B. Y. (1984). ''Torsion of a long cylindrical elastic bar partially embedded in layered elastic half space.'' *Int. J. Solids and Struct.*, 20, 1–11.

Luk, V. K., and Keer, L. M. (1979). ''Stress analysis for an elastic half space containing an axially loaded rigid cylindrical rod.'' *Int. J. Solids and Struct.*, 15, 805–827.

Muki, R., and Sternberg, E. (1969). ''On the diffusion of an axial load from an infinite cylindrical bar embedded in an elastic medium.'' *Int. J. Solids and Struct.*, 5, 587–606.

Muki, R., and Sternberg, E. (1970). ''Elastostatic load transfer to a half space from a partially embedded axially loaded rod.'' *Int. J. Solids and Struct.*, 6, 69–90.

Niumpradit, B., and Karasudhi, P. (1981). ''Load transfer from an elastic

pile to a saturated porous elastic soil.'' *Int. J. Numer. and Analytical Methods in Geomech.*, 5, 115–138.
Philippacopoulos, A. J. (1988). ''Lamb's problem for fluid-saturated porous media.'' *Bull. Seismological Society of Am.*, 78, 908–923.
Rajapakse, R. K. N. D. (1988a). ''A note on the elastodynamic load transfer problem.'' *Int. J. Solids and Struct.*, 24, 963–972.
Rajapakse, R. K. N. D. (1988b). ''Dynamics of piles: A critical evaluation of continuum solution models.'' *Proc., Annu. Conf. CSCE*, Vol. 3, 216–236.
Rajapakse, R. K. N. D., and Shah, A. H. (1987). ''On the longitudinal harmonic motion of an elastic bar embedded in an elastic half-space.'' *Int. J. Solids and Struct.*, 23, 267–285.
Selvadurai, A. P. S., and Rajapakse, R. K. N. D. (1987). ''Variational scheme for analysis of torsion of embedded non-uniform elastic bars.'' *J. Engrg. Mech.*, ASCE, 113, 1534–1550.

APPENDIX III. NOTATION

The following symbols are used in this paper:

a = radius of elastic bar;
E = drained Young's modulus of bulk material;
E_b = Young's modulus of elastic bar;
E_b^* = Young's modulus of fictitious bar;
h = length of elastic bar;
p_f = excess pore fluid pressure;
p_f^a = average pore pressure across D_z;
$p(z)$ = axial forces of elastic bar;
$p^*(z)$ = axial forces of fictitious bar;
u_r = radial displacement of solid matrix;
u_z = vertical displacement of solid matrix;
$w(z)$ = vertical displacement of D_z at $r = a$;
δ = nondimensional frequency of motion;
λ = Lamé's constant of bulk material;
μ = shear modulus of bulk material;
ν = Poisson's ratio of bulk material;
ρ = mass density of bulk material;
ρ_b = mass density of elastic bar;
ρ_f = mass density of pore fluid; and
ω = frequency of motion.